
Better Batch for Deep Probabilistic Time Series Forecasting

Vincent Zhihao Zheng, Seongjin Choi, Lijun Sun*

Department of Civil Engineering
McGill University
Montreal, QC H3A 0C3
zhihao.zheng@mail.mcgill.ca
seongjin.choi@mcgill.ca
lijun.sun@mcgill.ca

Abstract

Deep probabilistic time series forecasting has gained significant attention due to its ability to provide valuable uncertainty quantification for decision-making tasks. However, many existing models oversimplify the problem by assuming the error process is time-independent, thereby overlooking the serial correlation in the error process. This oversight can potentially diminish the accuracy of the forecasts, rendering these models less effective for decision-making purposes. To overcome this limitation, we propose an innovative training method that incorporates error autocorrelation to enhance the accuracy of probabilistic forecasting. Our method involves constructing a mini-batch as a collection of D consecutive time series segments for model training and explicitly learning a covariance matrix over each mini-batch that encodes the error correlation among adjacent time steps. The resulting covariance matrix can be used to improve prediction accuracy and enhance uncertainty quantification. We evaluate our method using DeepAR on multiple public datasets, and the experimental results confirm that our framework can effectively capture the error autocorrelation and enhance probabilistic forecasting.

1 Introduction

Time series forecasting has gained significant attention in the field of deep learning due to its wide-ranging applications [1]. Two primary types of forecasting tasks are deterministic forecasting and probabilistic forecasting. Deterministic forecasting provides point estimates for future time series values, while probabilistic forecasting goes a step further by providing a distribution that quantifies the uncertainty associated with the predictions. As the additional information about uncertainty aids decision-makers in making more informed decisions, probabilistic forecasting has become increasingly attractive, and extensive efforts have been made to enhance uncertainty quantification. In time series analysis, errors can exhibit correlation for various reasons, such as the omission of essential covariates or model inadequacy. Autocorrelation (also known as serial correlation) and contemporaneous correlation are two common types of correlation in multivariate time series forecasting. Autocorrelation captures the temporal correlation present in errors, whereas contemporaneous correlation refers to the correlation among different time series at the same time.

This paper primarily investigates the issue of autocorrelation in errors. Modeling error autocorrelation is a widely discussed topic, particularly in domains where model inference takes precedence over predictive performance. One common approach to tackle this issue is assuming that the errors of the base model follow an autoregressive (AR) process, with the residual errors assumed to be independent [2]. Similar challenges may arise in probabilistic forecasting, as current deep learning (DL)-based

models are typically trained without accounting for the autocorrelation of the error term. In this paper, we propose a novel batch structure that explicitly models error autocorrelation in probabilistic forecasting models. Each batch comprises multiple mini-batches, with each mini-batch grouping a fixed number of consecutive training instances. Previous studies have attempted to incorporate autocorrelation in deterministic time series forecasting by modifying the loss function through dynamic regression [3, 4]. However, since both the neural network and the correlated errors can explain the data, these models may face challenges in balancing the two sources in the absence of an overall covariance structure. Moreover, these methods are not readily applicable to probabilistic forecasting models, where the model’s output typically consists of parameters of the predictive distribution rather than the actual time series values.

Our main idea draws inspiration from the generalized least squares (GLS) method used in linear regression models with dependent errors. We extend the Gaussian likelihood of a univariate model to a multivariate Gaussian likelihood by incorporating a time-invariant covariance matrix that encodes error autocorrelation within a mini-batch. This covariance matrix is parameterized using a stationary kernel function, and its parameters are jointly learned with a base probabilistic forecasting model. This enables us to improve the accuracy of estimated distribution parameters during prediction by utilizing the learned covariance matrix to account for previously observed errors. By explicitly incorporating error correlation in the likelihood, our method facilitates more accurate training and prediction for time series data.

Our main contributions are:

- We propose a novel method that enhances the training and prediction of univariate probabilistic time series models by learning a covariance matrix that captures the autocorrelated errors within a mini-batch.
- We utilize a kernel function to parameterize the covariance matrix to ensure its positive definiteness. This approach enables us to jointly learn the parameters of the kernel function with the base model.
- Our method, based on DeepAR and evaluated on multiple datasets, effectively captures the autocorrelation in errors and improves prediction accuracy. Notably, these improvements are achieved through statistical formulation without significantly increasing the number of parameters in the model.

2 Preliminaries

2.1 Probabilistic time series forecasting

Denote $\mathbf{z}_t = [z_{1,t}, \dots, z_{N,t}]^\top \in \mathbb{R}^N$ the vector containing the values of a multivariate time series at time step t , where N is the number of time series. Given the observed history $\{\mathbf{z}_t\}_{t=1}^T$, Probabilistic time series forecasting can be formulated as estimating the joint conditional distribution $p(\mathbf{z}_{T+1}, \dots, \mathbf{z}_{T+Q} | \mathbf{z}_{T-P+1}, \dots, \mathbf{z}_T; \mathbf{x}_{T-P+1}, \dots, \mathbf{x}_{T+Q})$, where \mathbf{x}_t are some known time-dependent covariates (e.g., time of day and day of week). In other words, we are interested in forecasting Q futures values given P historical values and covariates. The model can be further factorized as

$$p(\mathbf{z}_{T+1}, \dots, \mathbf{z}_{T+Q} | \mathbf{z}_{T-P+1}, \dots, \mathbf{z}_T; \mathbf{x}_{T-P+1}, \dots, \mathbf{x}_{T+Q}) = \prod_{t=T+1}^{T+Q} p(\mathbf{z}_t | \mathbf{z}_{t-P}, \dots, \mathbf{z}_{t-1}; \mathbf{x}_{t-P}, \dots, \mathbf{x}_{t+Q-1}), \quad (1)$$

which is an autoregressive model that can be used for either one-step-ahead ($Q = 1$) or multi-step-ahead forecasting in a rolling manner. When used in multi-step ahead prediction, samples are drawn for the prediction range ($t \geq T + 1$) and fed back for the next time step until the end of the prediction range. The conditioning is usually encapsulated into a state vector \mathbf{h}_t of a transition dynamics f_Θ that evolves over time $\mathbf{h}_t = f_\Theta(\mathbf{h}_{t-1}, \mathbf{z}_{t-1}, \mathbf{x}_t)$. Therefore, Eq. (1) can be simplified as

$$p(\mathbf{z}_{T+1}, \dots, \mathbf{z}_{T+Q} | \mathbf{z}_{T-P+1}, \dots, \mathbf{z}_T; \mathbf{x}_{T-P+1}, \dots, \mathbf{x}_{T+Q}) = \prod_{t=T+1}^{T+Q} p(\mathbf{z}_t | \mathbf{h}_t), \quad (2)$$

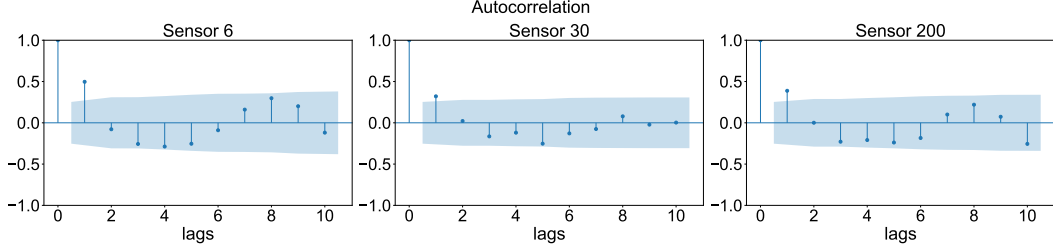


Figure 1: Error autocorrelation plot using one-step-ahead prediction results from DeepAR on the traffic dataset. The shaded area indicates the 95% confidence interval within which the correlation is statistically insignificant.

where we map \mathbf{h}_t to the parameters of a chosen parametric distribution (e.g., Gaussian, Poisson). When $N = 1$, the problem is reduced to a univariate model

$$p(\mathbf{z}_{i,T+1:T+Q} | \mathbf{z}_{i,T-P+1:T}, \mathbf{x}_{i,T-P+1:T+Q}) = \prod_{t=T+1}^{T+Q} p(z_{i,t} | \mathbf{h}_{i,t}), \quad (3)$$

where i is the identifier of a time series. This paper will focus on univariate models.

2.2 Error autocorrelation

In most probabilistic time series forecasting literature, the modeled data is often continuous and the errors are assumed to follow independent Gaussian distribution, i.e.,

$$z_{i,t} | \mathbf{h}_{i,t} \sim \mathcal{N}(\mu(\mathbf{h}_{i,t}), \sigma^2(\mathbf{h}_{i,t})), \quad (4)$$

where $\mu(\cdot)$ and $\sigma(\cdot)$ map the state vector $\mathbf{h}_{i,t}$ to the mean and standard deviation of a Gaussian distribution. For instance, the DeepAR model [5] adopts $\mu(\mathbf{h}_{i,t}) = \mathbf{w}_\mu^\top \mu(\mathbf{h}_{i,t}) + b_\mu$ and $\sigma(\mathbf{h}_{i,t}) = \log(1 + \exp(\mathbf{w}_\sigma^\top \mathbf{h}_{i,t} + b_\sigma))$ and both parameters are time-varying. This formulation is equivalent to decompose $z_{i,t} = \mu_{i,t} + \eta_{i,t}$ with $\eta_{i,t} \sim \mathcal{N}(0, \sigma_{i,t}^2)$. In the following of this paper, we focus on this setting with normally distributed errors. Assuming the errors to be independent corresponds to $\text{Cov}(\eta_{i,t-\Delta}, \eta_{i,t}) = 0, \forall \Delta \neq 0$.

When there exists serial correlation in the error process, we will have $\boldsymbol{\eta}_{T+1:T+Q} = [\eta_{i,T+1}, \dots, \eta_{i,T+Q}]^\top$ follows a multivariate Gaussian distribution with a certain covariance matrix $\mathcal{N}(\mathbf{0}, \boldsymbol{\Sigma})$, where $\boldsymbol{\Sigma}$ is the autocovariance matrix that has non-zero elements on its off-diagonal entries. Fig. 5 displays an example of error autocorrelation obtained through DeepAR on the traffic dataset for three sensors. The plot reveals a prevalent issue of lag-1 autocorrelation in traffic forecasting, even for one-step-ahead prediction.

3 Related Work

3.1 Probabilistic time series forecasting

Probabilistic forecasting aims to provide the probability distribution of the target variable instead of generating a single point estimate as in deterministic forecasting. Essentially, there are two approaches to achieve this, through the probability density function (PDF) and through the quantile function [1]. For instance, MQ-RNN [6] directly generates quantile forecasts using a sequence-to-sequence (Seq2Seq) recurrent neural network (RNN) architecture. The PDF-based approaches, which are widely used, often assume a specific distribution form for the target variables and utilize neural networks to generate the parameters of the distribution. DeepAR [5] is a notable example that employs an RNN architecture to model hidden state transitions. At each time step, the hidden state is used to conditionally generate the parameters of a Gaussian distribution, from which prediction samples are drawn. DeepVAR [7], the multivariate version of DeepAR, utilizes Gaussian copula to construct a joint cumulative distribution by mapping the original variables to marginally uniform variables. In addition to outputting distribution parameters, neural networks can be used to generate

probabilistic model parameters. For instance, deep state space model (SSM) [8] utilizes RNNs to generate SSM parameters, enabling the generation of prediction samples. Normalizing Kalman Filter (NKF) [9] combines normalizing flows (NFs) with the classical linear Gaussian state space model (LGM) to model non-linear dynamics and evaluate the probability density function of observations. The RNNs in the NKF model generate the parameters at each time step. Deep factor model [10] consists of a fixed global component and a random component, which can be any classic probabilistic time series model such as a Gaussian noise process. The global component, parameterized by neural networks, combines deterministic factors, while the random component forms the latent function that conditions a parametric distribution to generate observations. Some approaches aim to provide more expressive conditioning for probabilistic forecasting, such as using Transformer to replace RNNs to model the dynamics of latent states, thus breaking the Markovian assumption in RNNs [11]. This allows for more complex dependencies and improved forecasting performance. We refer readers to [1] for a recent and comprehensive review.

3.2 Modeling correlated errors

The issue of error correlation in time series data has been extensively studied in the fields of econometrics and statistics [12, 2, 13]. Autocorrelation, also known as serial correlation, captures the correlation of errors over time in a univariate time series. Contemporaneous correlation refers to the correlation among a set of time series variables at the same time period. Statistical frameworks, such as autoregressive (AR) and moving average (MA) models, along with their multivariate counterparts, have been well-developed in statistics to address these correlation issues. Several recent DL-based time series models have also tried to explicitly model error correlation structures to enhance forecasting performance. For example, to model serial correlation, in [3], the input and output of a neural network are parameterized to model first-order error autocorrelation in time series, thus capturing serially correlated errors with an autoregressive (AR) process. This technique enhances the performance of DL-based one-step-ahead forecasting models, enabling joint optimization of the base and error regressors. The method has been extended to multivariate models for Seq2Seq time series forecasting tasks, assuming a matrix AR process for the error matrix [4]. In terms of learning contemporaneous correlation, researchers have proposed modeling error correlation using a multivariate Gaussian distribution in node regression problems [14]. The resulting method, called error propagation in Graph Neural Networks (GNNs), adjusts the prediction of unknown nodes based on known node labels. Similarly, a correct-and-smooth model was proposed for classification tasks, correcting correlated errors in GNNs [15]. Generalized Least Squares (GLS) loss is introduced in [16] to capture error spatial correlation in neural networks for geospatial data, which bridges deep learning with Gaussian processes. In [17], a dynamic mixture of matrix normal distributions was proposed to characterize the multidimensional spatiotemporal correlation of errors in Seq2Seq models.

To the best of our knowledge, our work is the first to address the problem of error autocorrelation in probabilistic time series forecasting by designing new training schemes. Our proposed method is closely related to the methods presented in [3] and [16]. Compared to [3], our method focuses on learning a covariance matrix for a mini-batch with autocorrelated errors rather than learning regression coefficients for an error AR process. The introduction and learning of the error covariance matrix not only offer a statistically consistent framework but also enable more accurate prediction. In comparison to the GLS scheme in [16] for spatial interpolation/kriging, our method learns correlation over the temporal dimension to enhance forecasting.

4 Our Method

Our method is based on the formulation in Eq. (3), with DeepAR [5] serving as a base model. DeepAR is a global univariate model based on autoregressive recurrent neural networks. The model uses RNNs to describe the transition in states \mathbf{h}_t , and the encoder-decoder framework is used to map an input sequence of P time steps to an output sequence of Q time steps. The state $\mathbf{h}_{i,t}$ is used to output the parameters θ of a fixed distribution. The likelihood is given by $p(z_{i,t} | \theta(\mathbf{h}_{i,t}))$, where a Gaussian distribution is employed, i.e., $\theta(\mathbf{h}_{i,t}) = (\mu_{i,t}, \sigma_{i,t})$. In the training batch, the target time series variable can be modeled as

$$z_{i,t} = \mu_{i,t} + \sigma_{i,t}\epsilon_{i,t}. \tag{5}$$

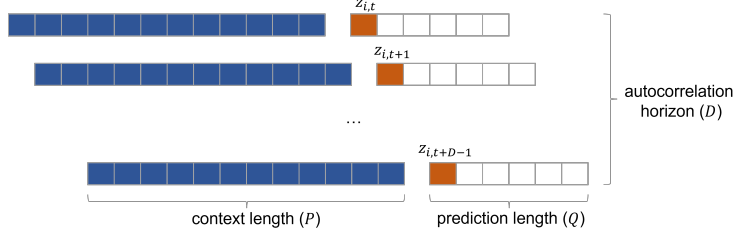


Figure 2: Example of a mini-batch. Colored parts denote the time series segments that construct the mini-batch. Each mini-batch has a time span of $P + D$, and only one-step-ahead prediction is involved during the training.

The Gaussian likelihood-based DeepAR model is built on the assumption that $\epsilon_{i,t} = \frac{z_{i,t} - \mu_{i,t}}{\sigma_{i,t}} \stackrel{\text{iid}}{\sim} \mathcal{N}(0, 1)$, implying that $\sigma_{i,t}$ are independent and identically distributed according to a standard normal distribution. Model training can be achieved by maximizing the log-likelihood

$$\mathcal{L} = \sum_{i=1}^N \sum_{t=1}^T \log p(z_{i,t} | \theta(\mathbf{h}_{i,t})) \propto \sum_{i=1}^N \sum_{t=1}^T -\frac{1}{2} \epsilon_{i,t}^2 - \ln \sigma_{i,t}, \quad (6)$$

Additionally, if we assume the error process to be isotropic, the loss function is equivalent to the Mean Squared Error (MSE) used in training deterministic forecasting models [3]. However, this assumption of independence disregards the potential serial correlation in $\epsilon_{i,t}$.

4.1 Training with mini-batch

We propose a novel training approach by constructing mini-batches instead of using individual training instances. For most existing deep probabilistic time series models including DeepAR, each training instance consists of a time series segment with a length of $P + Q$, where P represents the context length and Q denotes the prediction length. However, as mentioned, this simple approach cannot characterize the serial correlation of errors among consecutive time instances/steps. To address this issue, we group D consecutive time series segments into a mini-batch, with each segment having a length of $P + 1$ (i.e., $Q = 1$). The composition of a mini-batch is illustrated in Fig. 2. Although our training approach focuses on one-step-ahead prediction, it is equivalent to the conventional method that employs teacher forcing to forecast D future steps, as the prediction start times are aligned within each mini-batch. An example of the collection of target variables in a mini-batch of size D (the time horizon we use for capturing serial correlation) is given by

$$\begin{aligned} z_{i,t} &= \mu_{i,t} + \sigma_{i,t} \epsilon_{i,t}, \\ z_{i,t+1} &= \mu_{i,t+1} + \sigma_{i,t+1} \epsilon_{i,t+1}, \\ &\dots \\ z_{i,t+D-1} &= \mu_{i,t+D-1} + \sigma_{i,t+D-1} \epsilon_{i,t+D-1}, \end{aligned} \quad (7)$$

where $\mu_{i,t}$ and $\sigma_{i,t}$ are the outputs of DeepAR for each time series segment in the mini-batch, $\epsilon_{i,t}$ is the error term. As DeepAR is a univariate model, we omit the subscript i for the remainder of this paper. We use boldface symbols to denote the vectors of data and parameters in this mini-batch, e.g., $\mathbf{z}_t^{\text{bat}} = [z_t, z_{t+1}, \dots, z_{t+D-1}]^\top$ and the same notation applies to $\boldsymbol{\mu}_t^{\text{bat}}$ and $\boldsymbol{\sigma}_t^{\text{bat}}$.

Rather than assuming independence among the normalized errors ϵ_t , we consider the joint distribution of the error vector in a mini-batch $\boldsymbol{\epsilon}_t$, denoted as $\boldsymbol{\epsilon}_t^{\text{bat}} = [\epsilon_t, \epsilon_{t+1}, \dots, \epsilon_{t+D-1}]^\top \sim \mathcal{N}(\mathbf{0}, \mathbf{C})$, where \mathbf{C} is a time-invariant covariance matrix. We parameterize \mathbf{C} as $\mathbf{C} = (1 - v)\mathbf{K} + v\mathbf{I}$, where $v \in (0, 1)$. Here, \mathbf{K} is a covariance matrix generated from a squared-exponential (SE) kernel function, $\mathbf{K}^{ij} = \exp(-\frac{(i-j)^2}{l^2})$. Thus, we have $\mathbf{C}^{ij} = (1 - v) \exp(-\frac{(i-j)^2}{l^2}) + v\delta(i - j)$, where $\delta(\cdot)$ represents the Dirac delta function. Consequently, \mathbf{C} is a valid covariance matrix as \mathbf{K} originates from a kernel function. As the diagonal entries of \mathbf{C} remain 1, the marginal distribution of ϵ_t remains a standard normal distribution, and we can consider \mathbf{C} to be a correlation matrix. By treating v as a trainable parameter jointly optimized with DeepAR, we can capture the desired correlation structure within a mini-batch. A smaller value of v leads to a more correlated error process, while a larger

value corresponds to a more independent error process. This parameterization allows us to capture positive autocorrelation that decays over time lags. Alternatively, one could employ a moving-average process, such as $MA(q)$, to parameterize the correlation matrix. This approach introduces additional parameters to be learned but enables flexible structure, e.g., capturing negative correlations.

With this formulation, the distribution of ϵ_t becomes a multivariate Gaussian, which also leads to a multivariate Gaussian distribution for the target variables $z_t^{\text{bat}} \sim \mathcal{N}(\mu_t^{\text{bat}}, \Sigma_t^{\text{bat}})$. The $D \times D$ covariance of the associated target variables can be decomposed as $\Sigma_t^{\text{bat}} = \text{diag}(\sigma_t^{\text{bat}})C \text{diag}(\sigma_t^{\text{bat}})$. As both μ_t^{bat} and σ_t^{bat} are outputs of DeepAR, the likelihood for a specific time series i can be constructed for each mini-batch, and the overall likelihood is given by:

$$\mathcal{L}_i = \sum_{t=1}^{T-D+1} \log p(z_t^{\text{bat}} | \mu_t^{\text{bat}}, \Sigma_t^{\text{bat}}). \quad (8)$$

By allowing overlap, $T - D + 1$ mini-batches can be generated from the training data. It is worth emphasizing that the formulation assumes a time-invariant and stationary correlation matrix C . However, it can still capture a time-varying distribution through the varying values of μ_t^{bat} and σ_t^{bat} obtained from the neural network.

4.2 One-step-ahead forecasting and multi-step rolling forecasting

DeepAR performs forecasting in a rolling manner, i.e., a sample of the target variable is drawn at each time step and fed to the next time step as input until reaching the desired prediction range. Our method can provide extra calibration for this process given the learned correlation matrix C . Assume that we have observations till time step t and recall the collection of normalized error in a mini-batch jointly follows a multivariate Gaussian. Thus, for the first time step ($t + 1$) to be predicted, we have the conditional distribution of ϵ_{t+1} given the past $D - 1$ observed errors:

$$\epsilon_{t+1} | \epsilon_t, \epsilon_{t-1}, \dots, \epsilon_{t-D+2} \sim \mathcal{N}\left(C_* C_{\text{obs}}^{-1} \epsilon_t^{\text{obs}}, 1 - C_* C_{\text{obs}}^{-1} C_*^\top\right), \quad (9)$$

where $\epsilon_t^{\text{obs}} = [\epsilon_t, \epsilon_{t-1}, \dots, \epsilon_{t-D+2}]^\top \in \mathbb{R}^{D-1}$ is the collection of observed errors, which will be accessible/available when forecasting step $t + 1$. Here, C_{obs} corresponds to the $(D - 1) \times (D - 1)$ partition of C that describes the covariance within ϵ_t^{obs} , and C_* corresponds to the $1 \times (D - 1)$ partition of C that describes the covariance between ϵ_{t+1} and ϵ_t^{obs} , i.e., $C = \begin{bmatrix} C_{\text{obs}} & C_*^\top \\ C_* & 1 \end{bmatrix}$. As both μ_{t+1} and σ_{t+1} are deterministic output variables from DeepAR, we can first draw samples of ϵ_{t+1} from Eq. (9), and then transform them to target variable by

$$\tilde{z}_{t+1} = \mu_{t+1} + \sigma_{t+1} \tilde{\epsilon}_{t+1}, \quad (10)$$

where $\tilde{\epsilon}_t$ is a sample drawn from Eq. (9). As can be seen, the final distribution for z_{t+1} becomes

$$z_{t+1} | \mathbf{h}_{t+1}, \epsilon_t^{\text{obs}} \sim \mathcal{N}\left(\mu_{t+1} + \sigma_{t+1} C_* C_{\text{obs}}^{-1} \epsilon_t^{\text{obs}}, \sigma_{t+1}^2 \left(1 - C_* C_{\text{obs}}^{-1} C_*^\top\right)\right). \quad (11)$$

Following this approach, multi-step-ahead forecasting can be achieved in the same way as in DeepAR, by treating the sample $\tilde{\epsilon}_{t+1}$ as observation and continuing the process to get a trajectory of $\{\tilde{\epsilon}_{t+q}\}_{q=1}^Q$.

5 Experiments

5.1 Datasets and settings

We implement the proposed framework with DeepAR as the base prediction model. However, it should be noted that our approach can be applied to other autoregressive univariate models without any loss of generality, as long as the final prediction follows a normal distribution. To assess the effectiveness of our method, we conducted experiments on a diverse set of real-world datasets from GluonTS [18], including

- **traffic** [19]: This dataset contains the hourly traffic occupancy rate of the San Francisco freeway system between January 2008 and June 2008.

Table 1: Dataset and summary statistics.

Dataset	Granularity	# of time series	# of time steps	Context length	Testing horizon
traffic	hourly	963	4,025	24	30
electricity	hourly	370	5,857	24	30
m4-hourly	hourly	414	1,008	48	48
hospital	monthly	767	84	12	12
nn5	daily	111	791	56	56

- `electricity` [20]: It includes hourly electricity consumption data from 370 households between January 2012 and June 2014.
- `m4-hourly` [21]: This dataset consists of time series data from various fields, such as microeconomics, macroeconomics, finance, industry, demographics, and more. The data is derived from the M4-competition.
- `hospital` [22]: It comprises monthly counts of patients for different medical products associated with specific health issues recorded between 2000 and 2007.
- `nn5` [23]: This dataset contains daily cash withdrawal amounts from several ATMs across the UK, covering the period from March 1996 to May 1998. The data was used in the NN5 competition in 2008.

These datasets are widely used for benchmarking time series forecasting models. The statistics of all datasets are summarized in Table 1. We implement DeepAR using PyTorch Forecasting [24]. The testing horizon for each dataset was determined based on its configuration (i.e., the prediction length and the number of rolling evaluations) in GluonTS. For each dataset, we split it into training, validation, and testing sets in sequential order, with both the validation and testing sets being equal in size to the testing horizon shown in Table 1. Prior to being fed to the model, the data was normalized using the mean and standard deviation of the entire training set. The predictions were scaled back to the original scale to compute Continuous Ranked Probability Score (CRPS) as the evaluation metric.

In our implementation, we follow the configuration of the original DeepAR. The model takes as input the lagged time series values from the previous time step, along with additional features such as the time of day, day of the week, global time index, and identifier of each time series. The model architecture consists of three LSTM layers, each with a hidden size of 40. We used the Adam optimizer with a learning rate of 0.001 and terminated the training process when the loss on the validation set did not decrease for 10 epochs. Finally, we restore the best model parameters based on the validation set and use them to evaluate the model on the test set.

5.2 Evaluation against baseline

We conducted a comprehensive evaluation of our method by comparing it with the DeepAR model trained with Gaussian likelihood loss. To ensure a fair comparison in terms of the amount of data involved during training, we set the autocorrelation horizon (D) to be equal to the prediction length (Q). In our method, each mini-batch spans a time horizon of $P + D$, while in the conventional training method, each training instance spans a time horizon of $P + Q$. By setting $D = Q$, we ensured that both methods involve the same amount of data in a batch, given the same batch size. In practice, the prediction length is often set equal to the context length, i.e., $P = Q$. For simplicity, we set $Q = D = 12$ for all datasets. During the prediction stage, all models perform Q steps of rolling prediction.

Our proposed method introduces only two additional parameters to DeepAR: the lengthscale l of the squared exponential (SE) kernel and the weight parameter v used for generating the covariance matrix C . The lengthscale determines the decaying rate of the autocorrelation. Since autocorrelation typically persists over a few lags, in our experiments we consider l to be a hyperparameter and evaluate the performance for $l = 1, 2, 3$. For v , we parameterize it with a Sigmoid function and jointly optimize it with the base model.

In Table 2, we compare the prediction accuracy of different variants of DeepAR and demonstrate that our proposed method can improve the performance of DeepAR on all datasets across the prediction horizon when an appropriate lengthscale is chosen. It is worth noting that the optimal lengthscale can be determined by evaluating the performance on a validation set. While we present all the results

Table 2: CRPS accuracy comparison (lower is better, the best method is in bold). Mean and standard deviation were obtained by running each model three times.

Step	Datasets Models	traffic	electricity	m4-hourly	hospital	nn5
1	DeepAR	0.0059±0.0000	33.6583±0.1013	4.3925±0.0163	22.8855±0.0815	2.6443±0.0014
	+ $\mathcal{C}(l=1)$	0.0058±0.0000	35.3087±0.4350	3.7873±0.0085	17.4239±0.1731	2.6331±0.0012
	+ $\mathcal{C}(l=2)$	0.0061±0.0000	35.1775±0.3854	3.8117±0.0069	20.0910±0.1228	2.6344±0.0028
	+ $\mathcal{C}(l=3)$	0.0061±0.0000	34.6094±0.1912	3.9331±0.0038	15.6649±0.1201	2.6617±0.0039
3	DeepAR	0.0101±0.0000	49.4320±0.3697	7.4811±0.0051	31.2198±0.1793	2.8033±0.0006
	+ $\mathcal{C}(l=1)$	0.0088±0.0000	55.5005±0.9228	6.2640±0.0048	24.8251±0.1664	2.7905±0.0061
	+ $\mathcal{C}(l=2)$	0.0086±0.0000	52.5944±0.2460	6.3704±0.0211	37.9223±0.1975	2.7908±0.0040
	+ $\mathcal{C}(l=3)$	0.0091±0.0000	55.3385±0.2528	6.5917±0.0138	27.1259±0.2375	2.7986±0.0038
6	DeepAR	0.0106±0.0000	63.4259±0.4960	10.1670±0.0203	22.9670±0.0860	2.8063±0.0054
	+ $\mathcal{C}(l=1)$	0.0101±0.0000	67.7345±0.3425	8.5636±0.0035	18.9952±0.2706	2.7868±0.0026
	+ $\mathcal{C}(l=2)$	0.0087±0.0000	58.8421±0.1653	8.6556±0.0241	29.1139±0.0549	2.7818±0.0032
	+ $\mathcal{C}(l=3)$	0.0088±0.0000	61.2255±0.3736	8.9798±0.0105	22.5391±0.0983	2.8007±0.0048
9	DeepAR	0.0096±0.0000	73.7797±0.3031	10.7564±0.0093	21.8410±0.0861	2.7784±0.0025
	+ $\mathcal{C}(l=1)$	0.0086±0.0000	76.2201±0.3337	9.2220±0.0198	20.7420±0.0891	2.7819±0.0052
	+ $\mathcal{C}(l=2)$	0.0071±0.0000	62.3136±0.2971	9.1652±0.0200	24.4541±0.0759	2.7783±0.0040
	+ $\mathcal{C}(l=3)$	0.0072±0.0000	65.4184±0.3739	9.4689±0.0165	23.2547±0.0931	2.7772±0.0031
All	DeepAR	0.0100±0.0000	62.9288±0.0454	9.2121±0.0126	23.1338±0.0480	2.7878±0.0011
	+ $\mathcal{C}(l=1)$	0.0091±0.0000	66.1188±0.0942	7.8354±0.0023	21.1558±0.0740	2.7812±0.0011
	+ $\mathcal{C}(l=2)$	0.0079±0.0000	57.2124±0.2076	7.8612±0.0174	26.2640±0.0886	2.7812±0.0010
	+ $\mathcal{C}(l=3)$	0.0082±0.0000	59.6640±0.0585	8.1105±0.0041	22.6944±0.0933	2.7899±0.0014

here to examine the influence of the lengthscale, it is generally observed that the optimal l for the selected datasets is 1 or 2, indicating that the correlation generally exists within two lags.

We also evaluated the performance of our method considering different prediction steps (1/3/6/9-step-ahead predictions). Overall, our method consistently demonstrates effectiveness across these prediction steps. One notable advantage of our approach is its ability to mitigate the negative effects of accumulating errors over time. This is particularly evident in multiple datasets, such as `traffic`, `electricity`, and `m4-hourly`, where the accuracy improvement becomes increasingly significant as we extend the prediction further into the future. However, it is important to note that this pattern may not be as apparent in datasets with lower sampling rates, such as `hospital` and `nn5`, as prediction accuracy in such cases can depend greatly on the specific time periods considered. In the case of the `electricity` dataset, which exhibits high volatility, our method is outperformed by the baseline model at 1-step and 3-step prediction. Interestingly, the situation reverses for 6-step and 9-step prediction, where our method outperforms the baseline. This can be attributed to the fact that the baseline model, during training, only sums the individual Gaussian likelihood at each step over the prediction horizon, potentially leading to overfitting for near-step predictions. In the `nn5` dataset, the accuracy gain achieved by our method is limited, indicating a possibly weak error autocorrelation within the dataset (see Appendix B).

5.3 Interpretation of correlation

In this section, we present the correlation matrices learned from our proposed training method. One of the key advantages of our approach is that it guarantees the validity of the correlation matrix, including that the diagonal entries are equal to 1, all values lie within the range of -1 and 1, and the matrix is positive definite. Another advantage of our method is the inclusion of a trainable weight parameter v . Recall that errors in a mini-batch become more independent as v increases. When $v = 1$, the model reduces to the original DeepAR. This allows for additional control over the strength of the correlation between errors in a mini-batch, providing a way to fine-tune the model’s performance.

Table 3 provides an overview of the weight parameters learned using different lengthscales. It is interesting to note that, in general, the value of v increases as the lengthscale l increases. This trend can be attributed to the need to counterbalance the increased correlation strength for the same lag resulting from the kernel assumption. Additionally, the parameter v serves to scale the correlation strength for each specific dataset. For instance, the values of v tend to be larger in the `nn5` dataset compared to other datasets. This discrepancy arises due to the relatively weak error correlation present in `nn5`. In contrast, for the `m4` dataset, v is as small as 0.3257 for $l = 1$, suggesting that the lag-1 autocorrelation is particularly prominent in this dataset.

Table 3: Learned weight parameter (v) of each dataset (best model is in bold).

Datasets	traffic	electricity	m4-hourly	hospital	nn5
$v(l=1)$	0.5157	0.3713	0.3257	0.5199	0.7134
$v(l=2)$	0.6369	0.5494	0.5410	0.6150	0.7873
$v(l=3)$	0.6495	0.5927	0.5911	0.6302	0.8244

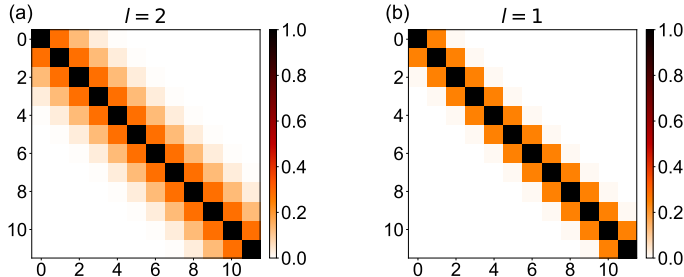


Figure 3: Learned correlation matrix with the optimal lengthscale of different datasets. (a) traffic; (b) m4-hourly. More plots can be found in Appendix C.

Fig. 3 presents the learned correlation matrices from two datasets. It is apparent from the figures that the lengthscale has a crucial role in controlling the time horizon over which autocorrelation occurs, whereas the weight parameter v functions as a scaling factor to diminish the correlation strength for all off-diagonal entries. Moreover, the correlation weakens swiftly after the lag identified by the lengthscale. For example, in the `traffic` dataset, the model takes into account approximately three previous errors when making predictions (Fig. 3 (a)). However, in the `m4-hourly` dataset, only the most recent error is considered during prediction (Fig. 3 (b)).

6 Conclusion and Broader Impacts

In conclusion, this paper introduces a novel method to tackle the issue of error autocorrelation in probabilistic time series forecasting. The method involves using mini-batches in training and learning a time-invariant covariance matrix that captures the correlation among normalized errors within a mini-batch. We implemented and evaluated the proposed method using DeepAR on various public datasets, demonstrating its effectiveness in significantly improving probabilistic forecasting by effectively capturing autocorrelation. The broader impact of our method can be observed in two aspects. Firstly, since Gaussian errors are commonly assumed in many probabilistic forecasting models, our method can be applied to enhance the training process of such models, potentially improving their performance across diverse applications. Secondly, the learned error autocorrelation can be leveraged to improve multi-step prediction by calibrating the distribution output at each forecasting step. This helps mitigate the increase in variance caused by error accumulation.

There are several directions for future research. First, the error autocorrelation structure is assumed to be subject-invariant and time-invariant, which may not hold for datasets with seasonal patterns and multivariate time series data with heterogeneous dynamics. To address this limitation, a time-varying correlation matrix could be employed (e.g., with time-varying weight v_t). Second, the kernel-based parameterization of the correlation matrix may be too restrictive for capturing temporal processes. Exploring more flexible autocorrelation structures, such as parameterizing C as a symmetric positive definite Toeplitz matrix, could be a promising avenue. Third, our method can be extended to multivariate models, in which the target output becomes a vector instead of a scalar. A possible solution is to use a matrix Gaussian distribution to replace the multivariate Gaussian distribution used in the current method. This would allow us to learn a full covariance matrix between different target series, thereby capturing any cross-correlations between them. Lastly, the idea of modeling autocorrelation can be extended to other distributions (e.g., Bernoulli and Poisson) within the exponential family, following the concept of the generalized linear model (GLM).

References

- [1] Konstantinos Benidis, Syama Sundar Rangapuram, Valentin Flunkert, Yuyang Wang, Danielle Maddix, Caner Turkmen, Jan Gasthaus, Michael Bohlke-Schneider, David Salinas, Lorenzo Stella, et al. Deep learning for time series forecasting: Tutorial and literature survey. *ACM Computing Surveys*, 55(6):1–36, 2022.
- [2] Rob J Hyndman and George Athanasopoulos. *Forecasting: Principles and Practice*. OTexts, 2018.
- [3] Fan-Keng Sun, Chris Lang, and Duane Boning. Adjusting for autocorrelated errors in neural networks for time series. *Advances in Neural Information Processing Systems*, 34:29806–29819, 2021.
- [4] Vincent Zhihao Zheng, Seongjin Choi, and Lijun Sun. Enhancing deep traffic forecasting models with dynamic regression. *arXiv preprint arXiv:2301.06650*, 2023.
- [5] David Salinas, Valentin Flunkert, Jan Gasthaus, and Tim Januschowski. Deepar: Probabilistic forecasting with autoregressive recurrent networks. *International Journal of Forecasting*, 36(3):1181–1191, 2020.
- [6] Ruofeng Wen, Kari Torkkola, Balakrishnan Narayanaswamy, and Dhruv Madeka. A multi-horizon quantile recurrent forecaster. *arXiv preprint arXiv:1711.11053*, 2017.
- [7] David Salinas, Michael Bohlke-Schneider, Laurent Callot, Roberto Medico, and Jan Gasthaus. High-dimensional multivariate forecasting with low-rank gaussian copula processes. *Advances in neural information processing systems*, 32, 2019.
- [8] Syama Sundar Rangapuram, Matthias W Seeger, Jan Gasthaus, Lorenzo Stella, Yuyang Wang, and Tim Januschowski. Deep state space models for time series forecasting. *Advances in neural information processing systems*, 31, 2018.
- [9] Emmanuel de Bézenac, Syama Sundar Rangapuram, Konstantinos Benidis, Michael Bohlke-Schneider, Richard Kurle, Lorenzo Stella, Hilaf Hasson, Patrick Gallinari, and Tim Januschowski. Normalizing kalman filters for multivariate time series analysis. *Advances in Neural Information Processing Systems*, 33:2995–3007, 2020.
- [10] Yuyang Wang, Alex Smola, Danielle Maddix, Jan Gasthaus, Dean Foster, and Tim Januschowski. Deep factors for forecasting. In *International conference on machine learning*, pages 6607–6617. PMLR, 2019.
- [11] Binh Tang and David S Matteson. Probabilistic transformer for time series analysis. *Advances in Neural Information Processing Systems*, 34:23592–23608, 2021.
- [12] Raquel Prado, Marco AR Ferreira, and Mike West. *Time Series: Modeling, Computation, and Inference*. CRC Press, 2021.
- [13] James Douglas Hamilton. *Time Series Analysis*. Princeton University Press, 2020.
- [14] Junteng Jia and Austion R Benson. Residual correlation in graph neural network regression. In *Proceedings of the 26th ACM SIGKDD International Conference on Knowledge Discovery & Data Mining*, pages 588–598, 2020.
- [15] Qian Huang, Horace He, Abhay Singh, Ser-Nam Lim, and Austin R Benson. Combining label propagation and simple models out-performs graph neural networks. *arXiv preprint arXiv:2010.13993*, 2020.
- [16] Wentao Zhan and Abhirup Datta. Neural networks for geospatial data. *arXiv preprint arXiv:2304.09157*, 2023.
- [17] Seongjin Choi, Nicolas Saunier, Martin Trepanier, and Lijun Sun. Spatiotemporal residual regularization with dynamic mixtures for traffic forecasting. *arXiv preprint arXiv:2212.06653*, 2022.
- [18] Alexander Alexandrov, Konstantinos Benidis, Michael Bohlke-Schneider, Valentin Flunkert, Jan Gasthaus, Tim Januschowski, Danielle C Maddix, Syama Rangapuram, David Salinas, Jasper Schulz, et al. Gluonts: Probabilistic and neural time series modeling in python. *The Journal of Machine Learning Research*, 21(1):4629–4634, 2020.
- [19] Caltrans. Caltrans performance measurement system. URL <https://pems.dot.ca.gov/>, 2015.

- [20] Dheeru Dua and Casey Graff. Uci machine learning repository. URL <https://archive.ics.uci.edu/ml/index.php>, 2017.
- [21] Spyros Makridakis, Evangelos Spiliotis, and Vassilios Assimakopoulos. The m4 competition: 100,000 time series and 61 forecasting methods. *International Journal of Forecasting*, 36(1):54–74, 2020.
- [22] Rob Hyndman, Anne B Koehler, J Keith Ord, and Ralph D Snyder. *Forecasting with exponential smoothing: the state space approach*. Springer Science & Business Media, 2008.
- [23] Souhaib Ben Taieb, Gianluca Bontempi, Amir F Atiya, and Antti Sorjamaa. A review and comparison of strategies for multi-step ahead time series forecasting based on the nn5 forecasting competition. *Expert systems with applications*, 39(8):7067–7083, 2012.
- [24] Jan Beitner. Pytorch forecasting. URL <https://pytorch-forecasting.readthedocs.io/en/stable/>, 2023.

Appendix

A. Datasets

Appendix A provides example time series plots for each of the datasets used in our experiment (Fig. 4). It is important to note that the scales for each series may vary greatly, even within the same dataset.

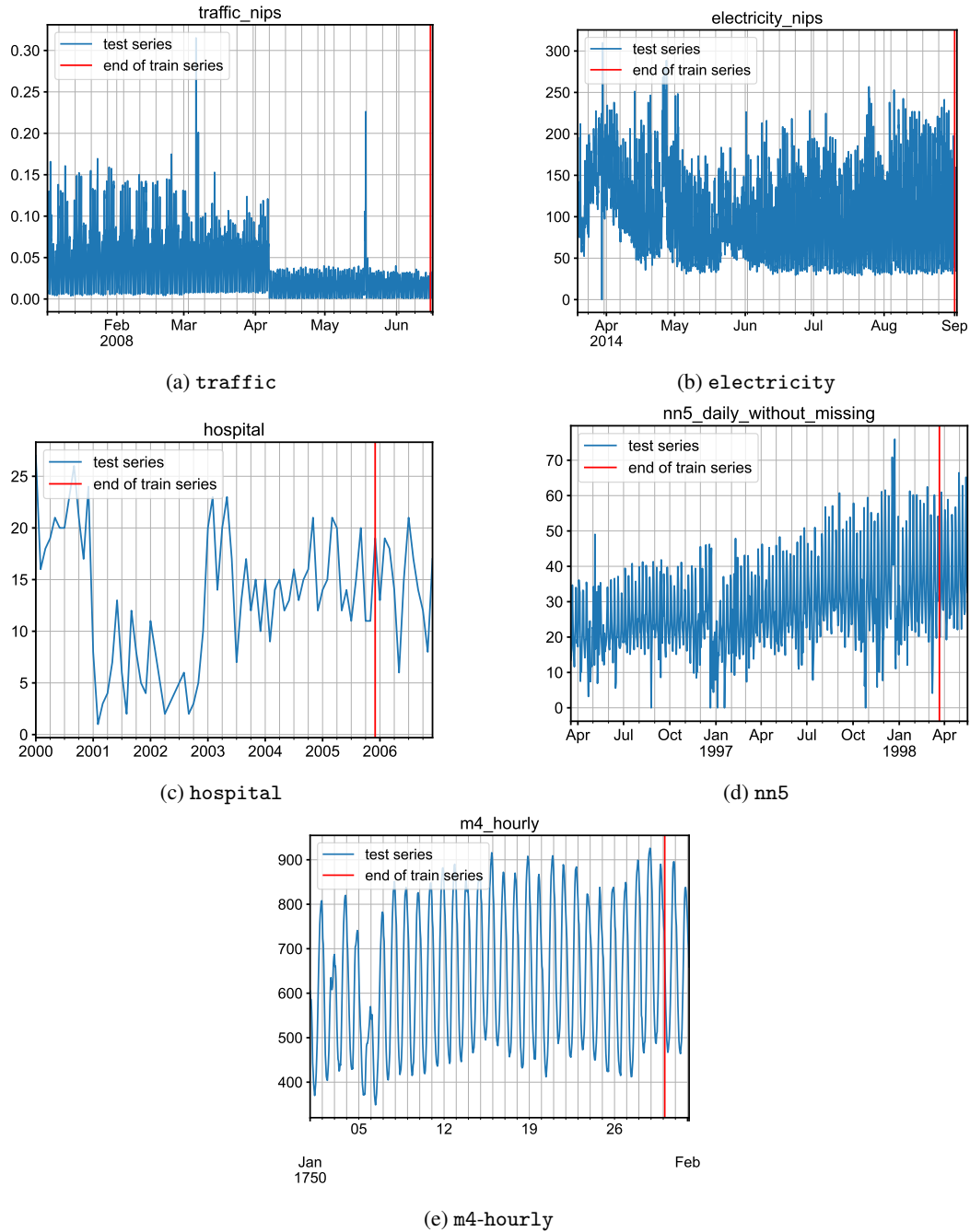


Figure 4: Example time series from each dataset.

B. Error autocorrelation

Appendix B presents additional examples of error autocorrelation plots from each dataset using DeepAR trained with one-step-ahead prediction loss (Fig. 5-9). It is worth noting that autocorrelation patterns can differ significantly from one time series to another within the same dataset. It is evident that the error autocorrelation in nn5 is considerably weak, resulting in limited improvement achieved by our method (Fig. 8).

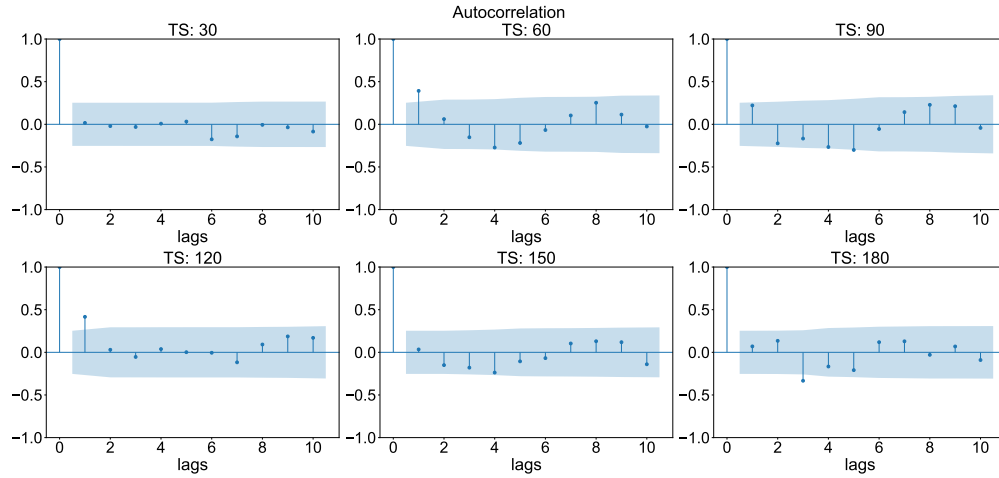


Figure 5: Autocorrelation plot of errors from one-step DeepAR model on the traffic dataset.

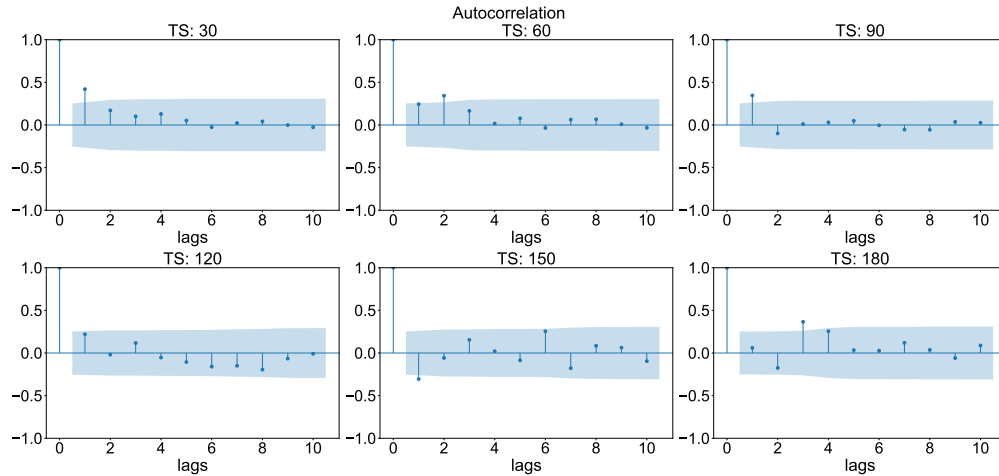


Figure 6: Autocorrelation plot of errors from one-step DeepAR model on the electricity dataset.

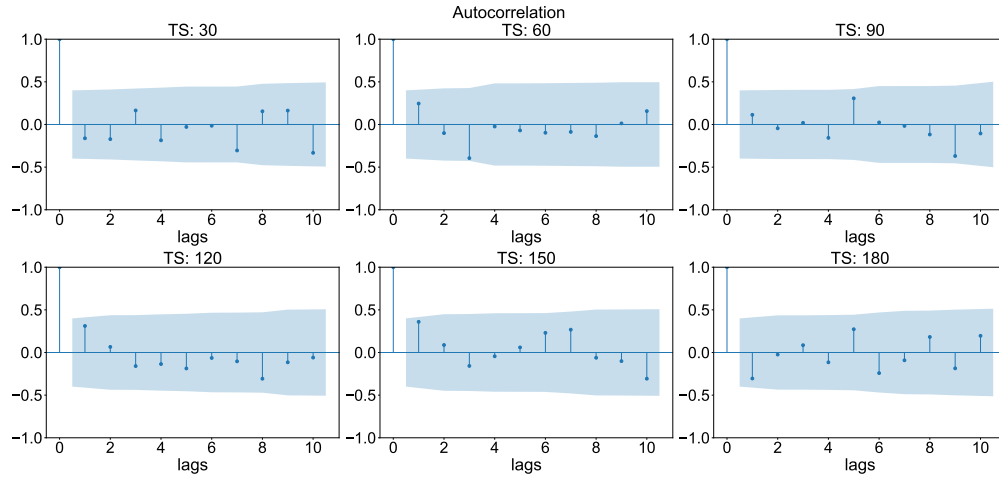


Figure 7: Autocorrelation plot of errors from one-step DeepAR model on the hospital dataset.

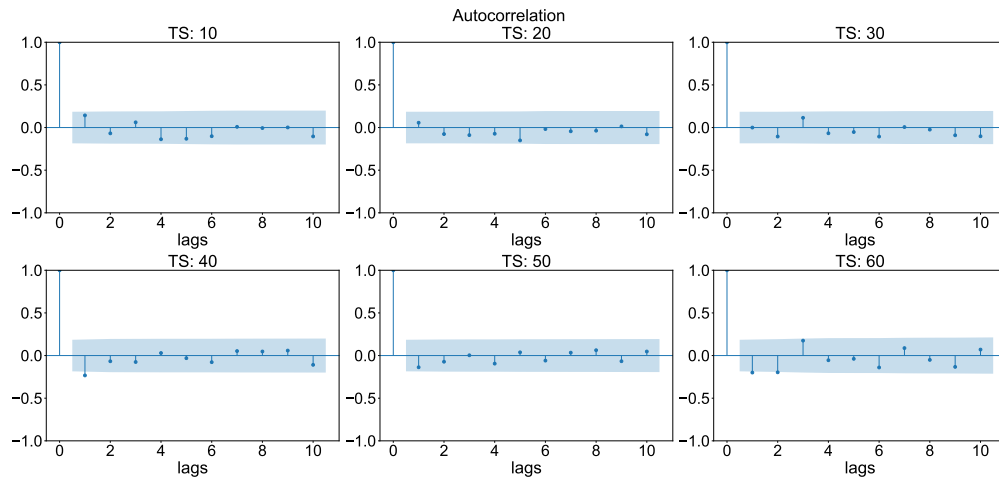


Figure 8: Autocorrelation plot of errors from one-step DeepAR model on the mn5 dataset.

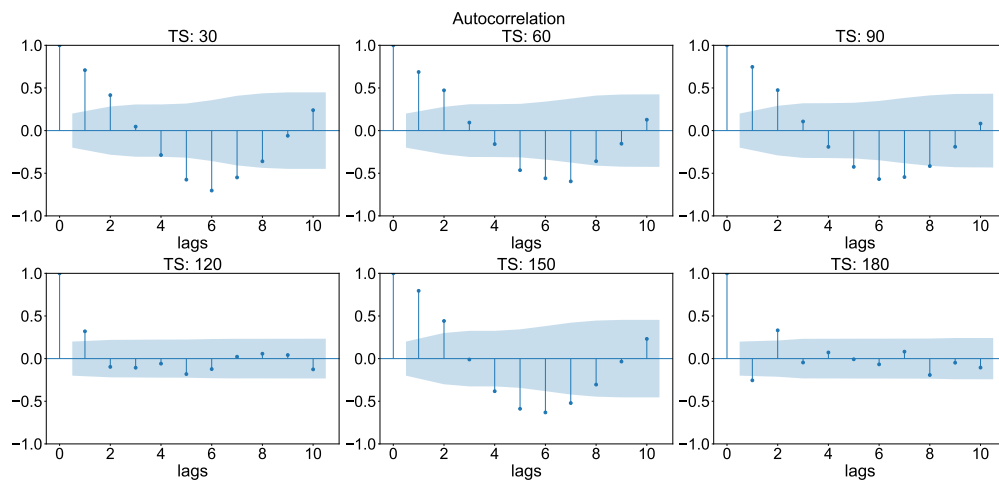


Figure 9: Autocorrelation plot of errors from one-step DeepAR model on the m4-hourly dataset.

C. Learned correlation matrix

Appendix C presents all correlation matrices learned from different datasets, each with varying lengthscales (l). It is apparent that l primarily determines the decaying rate of the autocorrelation, while v scales down the correlation strength.

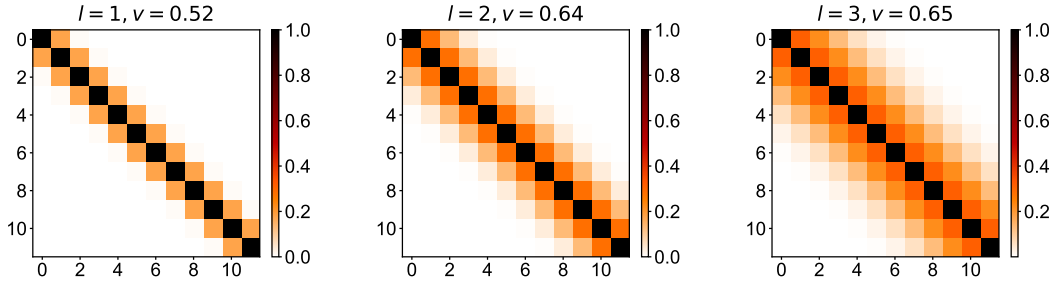


Figure 10: Correlation matrices for the traffic dataset.

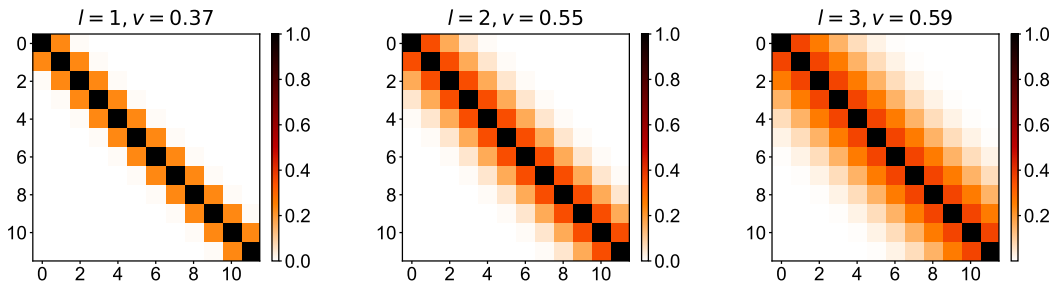


Figure 11: Correlation matrices for the electricity dataset.

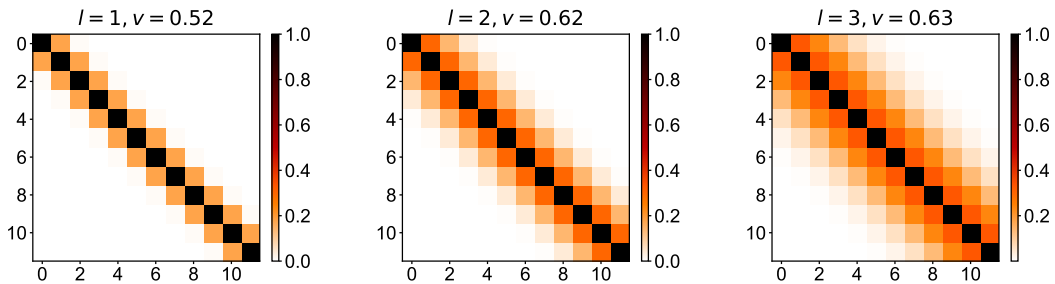


Figure 12: Correlation matrices for the hospital dataset.

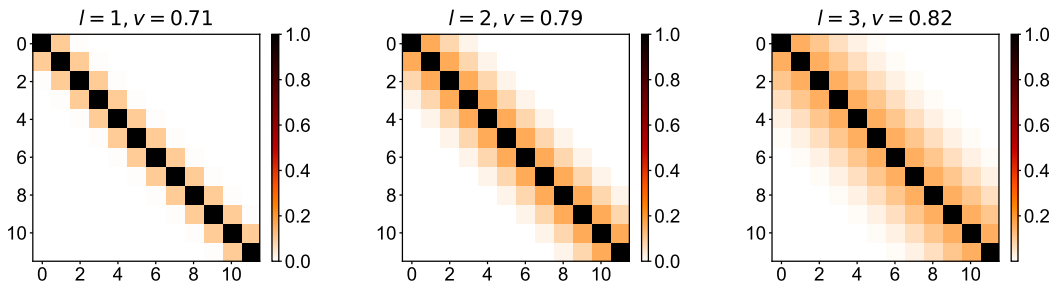


Figure 13: Correlation matrices for the nn5 dataset.

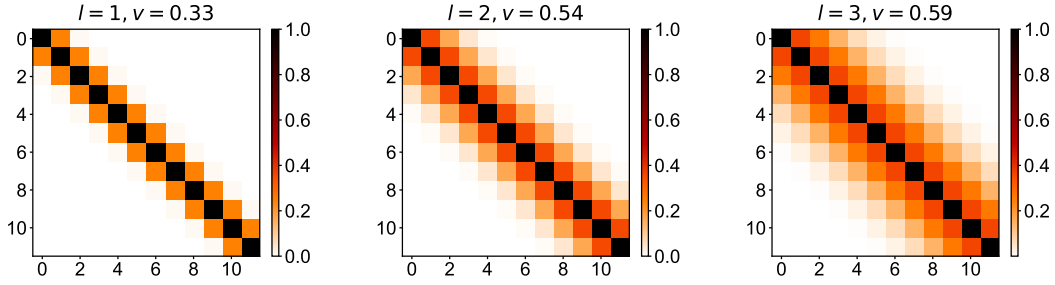


Figure 14: Correlation matrices for the m4-hourly dataset.

D. Prediction results

Appendix D showcases examples of prediction plots for various datasets using our method, including different quantiles (2%, 10%, 25%, 50%, 75%, 90%, and 98%) of the sampled predictions. Time step 0 separates the context and prediction range.

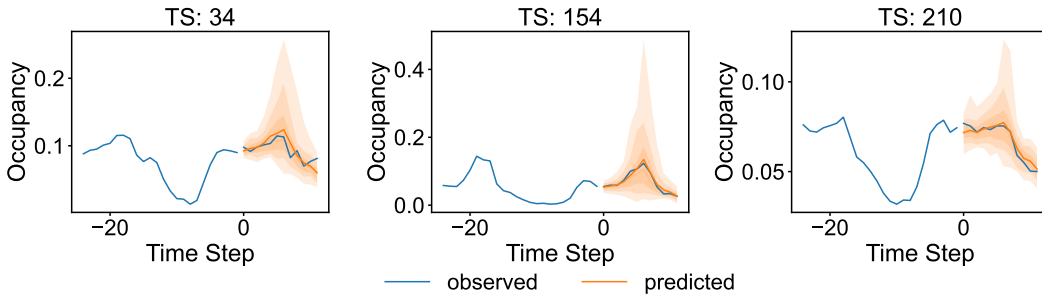


Figure 15: Prediction plots of traffic with our method ($l = 2$).

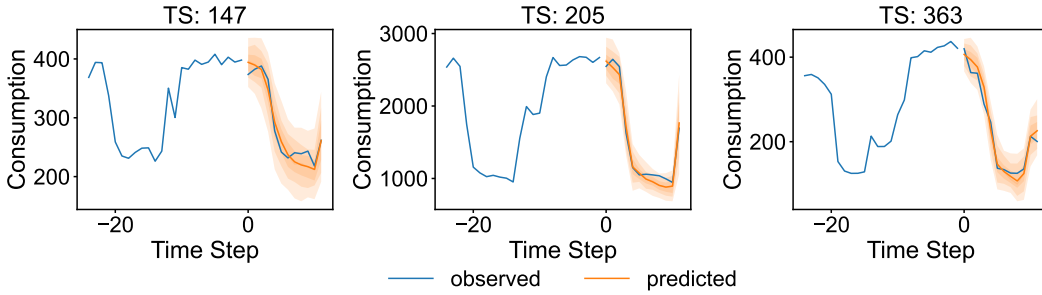


Figure 16: Prediction plots of electricity with our method ($l = 2$).

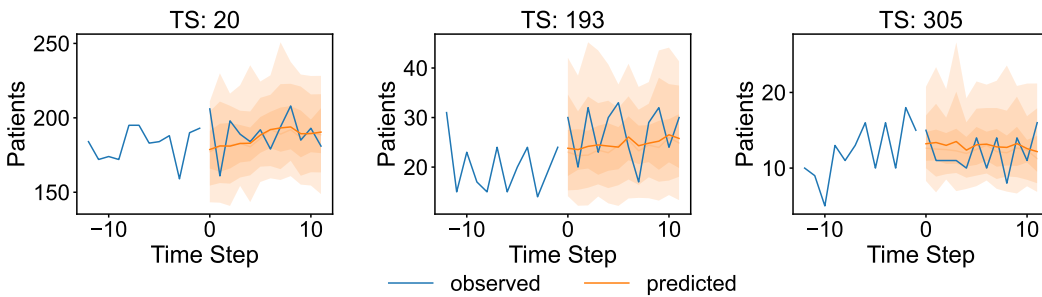


Figure 17: Prediction plots of hospital with our method ($l = 1$).

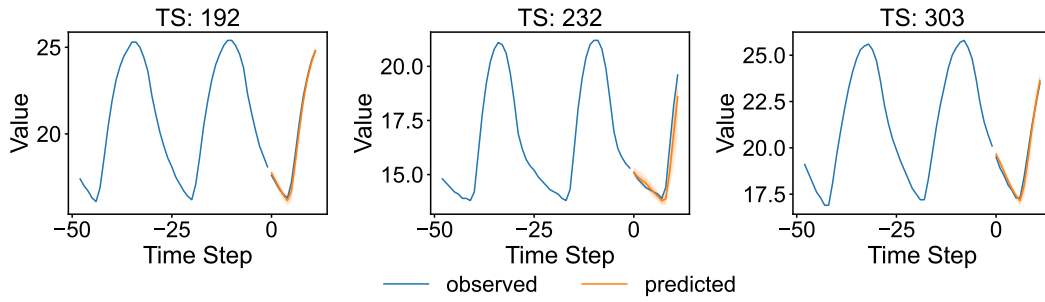


Figure 18: Prediction plots of m4-hourly with our method ($l = 1$).

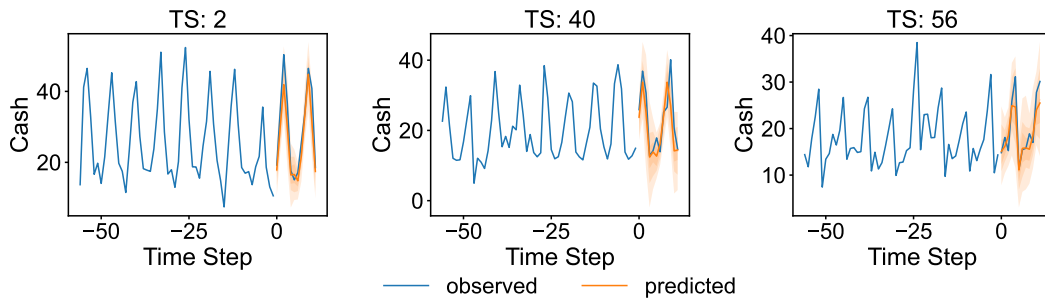


Figure 19: Prediction plots of nn5 with our method ($l = 2$).